DOI: 10.13009/EUCASS2019-952

Thermal Challenges Related to Lunar In-Situ Resources Utilization: Analysis of a Regolith Mining System

Lorenzo Rabagliati*, Manohar Karnal**, Paolo Pino***, Stefano Bertolotto****, Shrrirup Nambiar*****, Corentin Buti******

*Politecnico di Torino - Corso Duca degli Abruzzi 24, I-10129, Torino, Italy
rabagliati.lorenzo@gmail.com

**Politecnico di Torino - Corso Duca degli Abruzzi 24, I-10129, Torino, Italy
karnal1988@gmail.com

***Politecnico di Torino - Corso Duca degli Abruzzi 24, I-10129, Torino, Italy
paolopino94@gmail.com

****Politecnico di Torino - Corso Duca degli Abruzzi 24, I-10129, Torino, Italy
s.bertolotto92@gmail.com

*****Politecnico di Torino - Corso Duca degli Abruzzi 24, I-10129, Torino, Italy
s266514@studenti.polito.it

******ISAE-Supaero - 10 Avenue Edouard Belin, 31400 Toulouse, France
Corentin.BUTI@isae-supaero.fr

Abstract
This paper discusses how the extreme thermal conditions of the Moon south pole region affect the design of a regolith mining systems for in situ resource utilisation purpose. This means dealing with temperatures possibly lower than 40 K. A hybrid thermal control system designed to withstand such thermal loads is here described. This design is assessed in parallel with thermal analyses, of which the preliminary results are presented. Particular focus is given to the technology enhancements required to enable such a mission, energy storage and mechanisms being the most critical ones.

Keywords: Thermal control system, Thermal analysis, In-situ resource utilisation, Extreme temperature environment, Lunar rover

1. Introduction

The permanent extension of human presence in the Solar System crucially depends on the ability of breaking the chain of Earth dependence, thus being able of exploiting other heavenly bodies resources. Part of this endeavour will consist in making space travel sustainable through in situ propellant production, in the crucial effort of tempering the burdens imposed by the rocket equation.
The present work addresses the topic of the thermal challenges related to the robotic extraction of icy regolith from the permanently shadowed regions (PSR) of the Shackleton Crater, in the lunar South Pole, as part of a wider plan aimed at producing liquid oxygen and liquid hydrogen from water electrolysis. This represents perhaps one of the major obstacles in achieving a successful exploitation of the lunar water reservoirs, due to the extremely hostile environment characterising the crater, with temperature as low as 25K.
Despite the importance of the problem, not many studies dealing with the possibility to explore the PSR on the Moon are present in literature. One of the few is Icebreaker, an exploration rover proposed by Dr. William Whittaker of Carnegie Mellon University [1]. The rest of the relevant literature (for instance [2], [3]) deals with missions that have to survive the lunar night, experiencing extremely low temperatures, however higher than the ones that are expected in the PSR. Hence, the aim of this paper is to fulfil this research gap by identifying a thermal control system (TCS) design capable of making robotic hardware survive in the extreme environment of PSR.
To begin with, the methodology employed in the project is briefly described. Then, the main inputs required for the analysis are reported, including a description of the mission, a research of the main environmental parameters affecting the thermal control of the system and the overall design of the system under study. Finally, TCS design and the results of the thermal analysis are discussed in details.

Copyright © 2019 by L. Rabagliati *et al*. Published by the EUCASS association with permission.

DOI: 10.13009/EUCASS2019-952

2. Methodology

The thermal control system (TCS) design described in this paper follows a standard approach, characteristic of preliminary phases of space mission design [4]. First of all, the inputs necessary for carrying out the study are collected:

- Mission requirements;
- Definition of orbits, which are relevant for the subsystem design;
- Timeline and load cases;
- Spacecraft geometry;
- Temperature limits, temperature gradients and temperature stability requirements;
- Properties of spacecraft equipment (i.e. thermal, mechanical, heat dissipation).

Afterwards, the TCS hardware design and analyses can start: firstly, the prediction of temperatures is obtained by solving the energy balance equation applied to the spacecraft; the temperatures predicted by the analysis, including margins, are then compared with the temperature requirements. If they are not fulfilled, the thermal hardware is modified until they are met. As a result, the design process is iterative and has as an output the spacecraft thermal hardware configuration and the spacecraft's temperature predictions [5].

3. Thermal control system: inputs

In the following sections, the aforementioned inputs are described in detail. The mission requirements and the timeline are presented together (Section 3.1). The definition of the orbits is here replaced by the description of the environment in which the system will work (Section 0). Then, the system design in terms of geometry, material selection and system level budgets are examined (Sections 3.3 and 3.4). Finally, the operating and non-operating temperatures for the equipment on board are reported (Section 3.5).

3.1. Concept of operations

The extraction of the regolith is performed by the Regolith Collection System (RCS), a rover designed to work in the Shackleton crater regions where water ice is present. The RCS operates in the context of a lunar propellant outpost aimed at generating and distributing propellant from lunar water. Icy regolith is extracted from the Shackleton crater PSR and transported to a propellant production facility deployed outside the crater. Here, water is separated from regolith and electrolysed, producing molecular hydrogen and oxygen. These gases are subsequently cooled down to their liquefaction temperatures and cryostored in order to be eventually distributed as cryogenic propellant, either on the surface or in cislunar space.

Coming back to the RCS rover, the large amount of regolith to be collected daily is assured by a swarm of RCSs. They mine in a designated area of 0.83 km^2 at 2.8 km from the Shackleton crater's edge. The mean slope between the crater's edge and the designated area is 31°, with a maximum value of 35.5°. Given the high slope of the crater, the rovers are transported by a motorised carriage. The carriage is moved using a Kevlar cable running from the vehicle itself to a motor on the crater's edge. Due to the high amount of regolith that has to be extracted in one day, a system of two carriages working in tandem is envisioned.

At the start of the working day, the swarm of RCSs is locked in position on top of the large carriage platform, close to the edge of the crater. The carriage moves to the rim of the crater with the help of the motor and descends along the slope. Upon reaching the mining area, the carriage ramp opens for the RCSs to disembark from the platform and to proceed with the mining operations. Once one RCS is full, it returns to the carriage and unloads regolith into the container. When the first carriage capacity is reached, it returns to the propellant production facility, while a second carriage goes down in to the crater to take back the second load and the swarm of RCSs.

On the edge of the crater, the carriages and the RCSs undergo the charging process lasting 5 hours and 8 hours respectively. The transfer time for the rovers and carriage from the rim to the designated area is 1 hour; the return trip takes 1.5 hours. The time allocated to the mining is 10 hours (Figure 1).

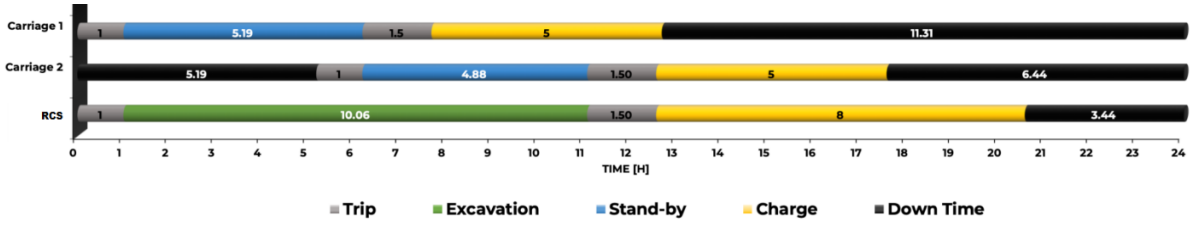

Figure 1: Operational timeline of regolith collection system and the carriage system

DOI: 10.13009/EUCASS2019-952

3.2. Shackleton Crater environment

Shackleton crater is located at $89.7°S$, $111°W$ [6]. Most of the interior lies in perpetual shadow, being located close to the south pole of the Moon, while the crater peaks are exposed to sunlight. Because of these unique properties, the crater plays a huge role in the lunar ISRU missions: it has been demonstrated [7] that the crater may trap and freeze the volatiles coming from comet impacts. For this reason, the Shackleton crater is believed to store ice regolith that can be extracted and used to produce propellant or for human mission on the lunar surface.
From the surface mapping of the Diviner Lunar Radiometer Experiment [8] it is possible to derive the temperature inside and outside the crater.

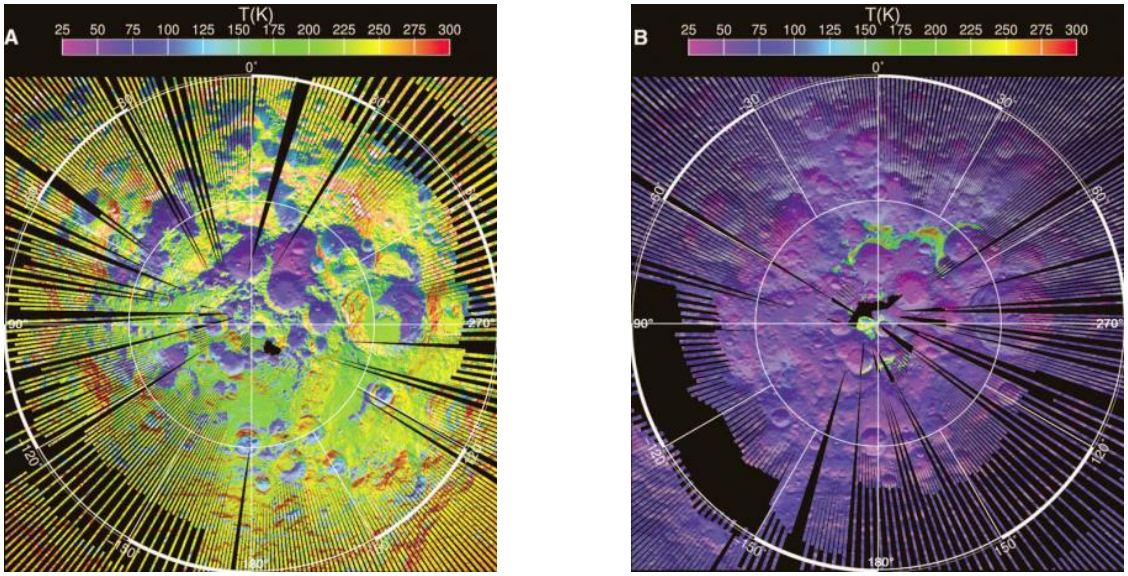

a) Day-time data b) Night-time data

Figure 2: Diviner-measured bolometric brightness temperatures [8].

Outside of the crater the temperature ranges from $75K$ to $250K$, while inside the temperature ranges from $25K$ to $75K$ (Figure 2). Since there is no detailed temperature profile available, the aforementioned data are taken as input for the preliminary thermal analysis.
In order to complete the set of necessary inputs regarding the environment, the thermo-optical properties of the lunar soil, i.e. regolith, have to be investigated.
On the lunar surface, the atmosphere is extremely thin and varies between 1.3×10^{-12} and $1.3 \times 10^{-14}\ mbar$ during lunar night and day respectively. Since gases are not present in significant amounts, the only contributions in heat exchange between the regolith and a lunar surface system are radiation and conduction. The radiative component can be divided into two main contributions: the solar direct heat flux and the heat emitted by the lunar surface. The albedo can be neglected in a first approximation, considering the Sun at an altitude of 0° on the horizon. Moreover, the thermal interface resistance between the surface and the system has to be addressed for the calculation of the conduction heat exchange between the rover and the lunar surface through the wheels' contact.
To summarise, emissivity, absorptivity and thermal interface resistance are the main properties that need to be identified in order to model the thermal coupling between the system and the surface.
The emissivity ε for regolith with a temperature between $90K$ and $400K$ was measured to be from 0.972 and 0.927 in an Apollo 11 sample with bulk density of 1910 kg/m^3 and 0.976 to 0.925 for an Apollo 14 sample with bulk density of 1600 kg/m^3. Based on these data, Birkebak and Cremers [9] fitted the spectral emissivity with a third order polynomial:

$$\varepsilon(T) = 0.9696 + 0.9664 \times 10^{-4}T - 0.31674 \times 10^{-6}T^2 - 0.50691 \times 10^{-9}T^3 \quad (1)$$

This formula is assumed to be valid also for the inner temperature of the crater, where $T < 90K$.
Regarding the absorptivity, it has been shown that it ranges between 0.703 and 0.924 [10]. The worst case values are thus taken for the thermal analysis.
Finally, the thermal interface conductance is important to estimate the heat load between the lunar surface and the rover's wheels. Usually, one can refer to experimental tables, but unfortunately, at the current state of writing, there

DOI: 10.13009/EUCASS2019-952

are no studies on the thermal interface conductance between metal faces and regolith. As a first estimation, the thermal interface conductance is adopted to be $h = 500\ Wm^{-2}K^{-1}$ [11].
Until now, the regolith has been considered as a solid layer over the outer shell of the Moon. However, the regolith is a porous media of rocks grained down to submicron size. Hence, regolith can easily float and cover the rover, modifying its thermo-optical properties, such as thermal conductivity, emissivity and absorptivity. In this paper, a preliminary analysis is conducted without taking into account this effect, nonetheless an interested reader may refer to Lieng-Huang [12].

3.3. RCS design

The work present in literature tackles different types of configurations for lunar exploration and excavation rovers [13]. The trade-off is carried out for four categories of excavators, namely discrete vs. continuous and heavy vs. lightweight ones. The Figures of Merit (FoM) considered are excavation time, power, mobility and payload ratio. Priority is given to the maximisation of the payload ratio, defined as the ratio between the amount of regolith collected and the dry mass of the system. Based on the trade-off results, bucket-drum system inspired from NASA Regolith Advanced Surface Systems Operations Robot (RASSOR) [14] are found to be an optimum solution.

The main mechanical design choices, affecting the system also on a thermal standpoint, are discussed below. Moreover, the material selection process for the main parts of the rover is described. The harsh lunar environment represents an extreme challenge for materials, whose selection is restricted to a limited area at the intersection between the operational circumstances and the functional performances. Temperature extremes and variations drive the strictest requirements, followed by relatively moderate demands on abrasion resistance. From a structural perspective, the low lunar gravity, along with proper design choices, would significantly play in favour of less compelling mechanical resistance needs, which would easily fall within those imposed by the launch phase.

Main body. The RCS is characterised by a single body design that was preferred to a multi-body articulated design. From a thermal point of view, this choice is driven by the fact that the heat losses due to the interconnecting elements are eliminated. Furthermore, from a configurational perspective, a multi-body design requires electrical and mechanical interconnections, thus reducing reliability and increasing complexity.
The body is represented by the warm electronics box (WEB), a structure that hosts vital subsystems of the rover and that combines thermal insulation features with structural properties. The need for structural strength and resistance to low temperatures justifies the adoption of aluminum honeycomb as structural material for the inner layer of the WEB (Section 4.2)
Composite materials have been investigated, but were eventually rejected due to their typical tendency in undergoing residual stresses at the interface between the matrix and the second phase, which would be further worsened by the continuous thermal and mechanical cycling over a wide range of temperatures.

Wheels. The rover is equipped with four elastic metal wheels with a $0.25\ m$ radius, $0.002\ m$ thick and $0.40\ m$ wide. Elastic wheels have a consolidated heritage in exploration rovers design and their mass can be reduced by introducing slots along the wheel circumference. For the present study, the size of the wheels is chosen as a preliminary measure to accommodate terrain irregularities, as shown in similar systems [14].
Different types of materials for wheels were taken into consideration. Due to temperature profiles and high radiation exposure, rubber tires shall be avoided, orienting the choice towards metallic, elastic tires. In particular, nickel-titanium shape memory alloys (SMA) represent one of the most accredited solutions for the design of future superelastic spring tires [15], thanks to their shape recovery and superelasticity properties. Furthermore, tuning Ni content would allow to engineer the transformation temperatures of the alloy to better meet the environmental conditions. However, little is known on the behaviour of the martensitic phase - in which the tire would be transformed into - during exposure to very low temperatures. For this reason, the choice for the elastic wheels material preliminary falls on Al 6061 T6 alloy. Aluminum wheels are also a flight proven technology that has been already used for the Curiosity Rover. The material selected for the wheel spokes is titanium, for its excellent specific mechanical properties and lower thermal conductivity with respect to aluminum, thus introducing higher resistance along the conductive paths between the rover body and the ground.

Suspensions. Suspensions are a critical part of the mechanical design, allowing the vehicle to rover across harsh terrains and to withstand the varying loads and mobility constraints imposed by the presence of obstacles and irregularities. On the flipside, their performances would be negatively impacted by low temperatures and dust that they would be easily exposed to. In addition to this, the actual existence of suspension systems capable of surviving this environment is still undocumented. Nevertheless, the need of suspensions in a lightweight system operating in lunar gravity can be questioned. Large, elastic wheels might accommodate obstacles scattered on the ground, while the relatively moderate stresses can be tolerated by structural parts even without energy dampers. Moreover, the concept of operation foresees a carriage mediating the transportation of the RCS swarm from the crater slope to the

DOI: 10.13009/EUCASS2019-952

propellant production facility, lowering the overall stress the rover will be subjected to. These reasons justify the initial selection of a simpler no-suspensions design.

Furthermore, the steering is achieved by applying more or less drive torque to one side of the vehicle by means of the motors placed inside the WEB. In fact, the more traditional configuration with driving motors inside the wheels and steering motors above is discarded because of the high exposure to the low temperature environment it would imply.

Bucket drums. The drums are both the regolith collection and the storage equipment and they have a maximum capacity of $30\ kg$ each. Supported on both sides by metallic arms, they are moved by one motor each and are characterised by an outer diameter of $0.25\ m$ and a width of $0.60\ m$.
Particular focus is given to the selection of the material of the bucket drums, which will be in direct contact with icy regolith during mining operations. One of the major concerns about materials arising in low temperature environments is the ductile-to-brittle transition. However, materials with a face-centred-cubic crystal structure, like aluminum and silver, are immune to this issue, presumably due to their higher availability of shear planes and directions. While some austenitic stainless steels might reveal a good solution [16], the higher specific strength and the vast heritage collected in aerospace engineering have led to the selection of aluminum alloys as deputy materials for the scooping equipment. In particular, Al 6061 T6 alloys result particularly promising for cryogenic applications below 50 K [17]. Robust mechanical resistance can be assured while retaining the required toughness. A more in-depth analysis of the operating conditions might induce the adoption of surface hardening treatments to improve wear resistance [18] or optical properties. Nevertheless, the scooping of small quantities of lunar regolith under reduced gravity definitely involves low stresses, thus avoiding the need for major expedients against microplaughing or other abrasive wear phenomena for a preliminary analysis.

Drums arms. The two arms connecting the WMBs to the rover body have a hollow rectangular cross section and they are made of the titanium alloy Ti - 5Al - 2.5Sn ELI. The lower thermal conductivity of this alloy with respect to aluminum alloys reduces the heat conduction between the excavating parts and the main body. Furthermore, this alloy is particularly recommended for cryogenic applications [17] and exhibits very good mechanical properties. Both Al 6061 T6 and Ti - 5Al - 2.5Sn Eli were selected also for their good weldability and the resistance of the welded joints, benefitting both design and operational performances.

Internal configuration. The internal configuration of the electronic hardware is crucial from the thermal control point of view. Each subsystem has its own operating and non-operating temperature requirements (Section 3.5) and power dissipation (Section 3.4), that end up in different suitable positions inside the warm electronics box. These drivers have resulted in the following configuration (Figure 3):

- the battery is placed in the centre of the rover body, on the bottom panel, surrounded by the rest of equipment that, dissipating power, protects it from low temperatures;
- the wheel and arm motors are placed besides the WEB walls, since they do not have strict temperature requirements and in order to reduce the distance between them and the mechanisms they have to move as much as possible;
- the rest of the different subsystem electronics is placed around the battery, but mounted on the top panel to be able to reject towards outside the heat dissipated when the subsystem is on.
- the drum motors are accommodated in two boxes, called warm motor boxes (WMB), that protect the motors from the external environment and are placed at the end of the arms.

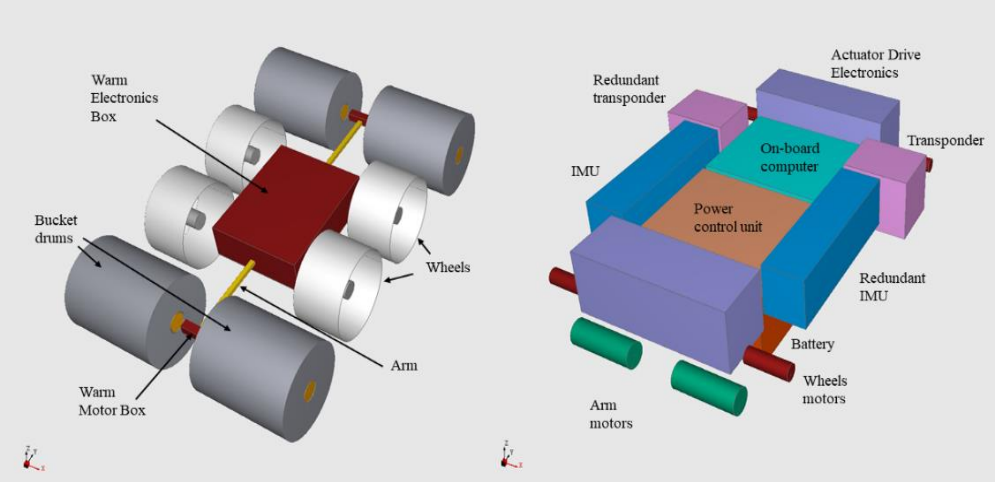

Figure 3: External and internal configuration of the RCS (thermal model)

DOI: 10.13009/EUCASS2019-952

3.4. System level budgets

The mass and power budget of the rover previously described are reported below, following ESA Margin Philosophy [19]. They are the results of a preliminary design also based on similar applications [1]. In the analysis, the power dissipation is considered, as a first assumption, to be equal to the electrical power demand.

Table 1: Mass budget of the RCS

Subsystem	Mass without margin [kg]	Design maturity mass margins	Mass with margin [kg]
Communication	8.0	10%	8.8
GNC	3.9	10%	4.3
OBC	2.0	10%	2.2
EPS	20.2	10%	22.2
Robotics	11.2	10%	12.4
Structure and Mechanisms	94.7	20%	113.6
TCS*	1.8	20%	2.2
Total mass without system level margin			165.7
System level margin		20%	33.1
Total mass with system level margin			198.8

*TCS figures are the output of the thermal analysis; WEB and WMBs are considered in Structure and Mechanisms.

Table 2: Power budget of the RCS

Subsystem	Nominal Moving [W]	Nominal Scooping [W]	Charging [W]	Standby [W]
Communication	20	2	2	2
GNC	20	20	2	2
OBC	6	6	6	1
EPS	6	6	6	1
Robotics	100	130	2	2
Structure and Mechanisms	0	0	0	0
TCS*	44	0	-	90
Total power without system level margin	196	164	18	98
System level margin (20%)	39	33	4	20
Total power with system level margin	235	197	22	118

*TCS figures are the output of the thermal analysis

3.5. Equipment operating and non-operating temperature

The mining rover and its subsystems presented in this paper have to survive an immensely harsh lunar environment (Section 0). These must not only be able to survive, but also to be highly reliable and operate at high efficiency throughout their operational life. The temperature requirements of the equipment depend on the technology used. As already stated, the main objective of the Thermal Control System (TCS) of the rover is to maintain the system and its subsystems working within their allowable temperature limits. The present state-of-the-art operating and non-operating temperature limits of the main system units are reported below (Table 3).

Table 3: Thermal requirements of the selected components

Equipment	Details	Operating temperature (°C)	Non-operating temperature (°C)
Energy storage devices	Li-ion Batteries [20], [21]	-40 to 85	-40 to 85
Motors	Maxon RE-25 [22]	-50 to 70	-120 to 80

DOI: 10.13009/EUCASS2019-952

Lubrication	Castrol Braycote 601 EF [23]	-80 to 204	-
General Electronics	(OBC, PDU, Comm, ADE) [24]	-45 to 60	-55 to 60
GNC	IMU [25]	-40 to + 50	-45 to 125

Table 3 shows the design temperature ranges. Following the ECSS standard [19], these temperatures must not be exceeded by the predicted temperature range obtained from the calculated temperature range increased by the uncertainties. The uncertainties of the analysis are related to many aspects of the thermal model such as complex view factors, material properties, radiation environment, joint and interface conduction, ground simulation etc. Usually, the uncertainties diminish as the project advance, since increasingly complex analyses, correlated to test results, are available. In this case, being a preliminary thermal analysis, $\pm 20°C$ of uncertainty margin is taken into account.

Also he uniformity and stability of the temperature required will have a significant impact on TCS design. Here, uniformity refers to maximum permissible temperature gradient within the subsystem and stability refers to the maximum variation of permissible temperature over a period of time for a definite item. The capability to meet these requirements is dependent on the power duty cycle, the environment to which the subsystem is exposed and the TCS design.
The tailoring of the equipment-structure mounting interface as well as the selection of the internal surface coatings and paints are crucial to obtain the required gradient of the temperature field inside the rover body (Section 4.2).

4. Thermal control system design

The RCS spacecraft Thermal Control System (TCS) is in charge of maintaining all spacecraft equipment within their allowed temperature ranges in all the possible scenarios.
The TCS shall fulfil the following objectives:

- to minimise the impact of the external environment on the rover equipment and subsystems;
- to control heat loads and heat leaks by tailoring conductive and radiative thermal exchanges;
- to prevent the ice from melting in the regolith of PSR by minimising radiative heating towards the lunar surface;
- to minimise heating power;
- to minimise hardware mass.

The TCS hardware designed to fulfil these objectives is described in the following sections.

4.1. Multi-layer insulation

The multilayer insulation is exploited to reduce the radiative heating towards the lunar surface, hence it covers completely the bottom panels of the WEB and the WMBs. In order to evaluate the MLI performance, the model proposed by Doenecke [26] is adopted. It consists in evaluating an effective emissivity ε_{eff} that takes into account both the radiative and the conductive coupling between the surface of the covered object and the outer layer of the MLI blanket. In the thermal analysis, this parameter allows to model the coupling between the surface of the object and the outer layer of the MLI blanket as if it were only radiative, thus avoiding to consider also a conduction link between them.
The effective emissivity is calculated as follows:

$$\varepsilon_{eff} = (0.000136/(4\sigma T_m^2) + 0.000121\, T_m^{0.667}) f_N f_A f_p \tag{2}$$

where T_m is the mean temperature calculated as

$$4T_m^3 = (T_h^4 - T_c^4)/(T_h - T_c) \tag{3}$$

with T_h and T_c the inner and outer MLI temperature respectively, expressed in K, while σ is the Stefan–Boltzmann constant, $f_p = 1$, $f_A = 1/10^{0.373 lnA}$, with A area of the blanket, and f_N depends on the layer density N. Since the optimum layer density depends on T_m, that affects in turns the overall effective emissivity, an iterative approach is adopted and the optimum value of 10 layers/cm is found, which gives $f_N = 1.425$ [26]. With the aforementioned values, the effective emissivity is $\varepsilon_{eff} = 2.3 \times 10^{-2}$, but since these values are not tested for temperatures lower than -140 K, which may be the case here, and the MLI theoretical model differs from the experimental values with an error up to 50%, an error of 100% is considered in the present analysis.

DOI: 10.13009/EUCASS2019-952

As regards the surface properties of the MLI blanket, the selected external coating is a Sheldahl aluminum coated polyimide film over-coated with silicon oxide, with emissivity $\varepsilon = 0.11$ [27].

4.2. Warm electronics box panels

The equipment at the heart of the rover is protected by a low conductivity, lightweight enclosure typically referred to as warm electronics box. The WEB is envisioned to combine structural and thermal insulation properties in order to withstand the mechanical loads while ensuring that the temperatures of the equipment inside are maintained within the operating limits. The resulting solution produces three different designs for the top, bottom and lateral panels of the box. The bottom panel facing the ground is designed to reduce the heat flux radiated outside so as to prevent the regolith from heating up. It is therefore constituted by a honeycomb structure made of an aluminum core and insulating carbon nanofibers composite facesheets [28]. On the external side, the surface is coated with the MLI already described (Section 4.1). On the internal side, the structure is cladded with a layer of silica aerogel, which is in turn covered with a low conductivity E glass fibers/epoxy composite sheet. Silica aerogel has a proven history of exceptional thermal insulation performance in space [29]. Due to the vacuum conditions, a thermal conductivity of $12 \times 10^{-3}\ W/m\,K$ [30] is used in sizing the insulation layer to accommodate the performances of the WEB. The aerogel is opacified to reduce the transmission of IR radiation across the wall. The glass-epoxy composite layer protects the underlying aerogel and offers a substrate to support the electronics. Finally, this surface is covered by a goldized kapton film that ensures additional retainment of the heat radiated by the equipment inside the box.

A similar configuration characterises the lateral panels, with few changes. Here, the innermost goldized kapton coating is replaced by a black painted kapton layer. The high emissivity value of this film (ε =0.92) allows to achieve more uniform temperatures. MLI is replaced by a surface coating with an emissivity ε = 0.4 and an absorptivity α = 0.3. These optical properties can be matched either by vacuum deposited silver and inconel backed teflon or by aluminised kapton [31]. However, teflon is recommended due to its thermal resistance ranging from -184 to 150°C [31].

Finally, the top panel is designed to achieve higher radiative heat exchanges with the external environment in order to avoid internal equipment overheating. This translates into replacement of the carbon composite facesheets covering the inner aluminium honeycomb core with more conductive aluminum facesheets. Moreover, both the silica aerogel and the glass-epoxy insulating layers are eliminated. Therefore, the honeycomb structure is internally coated with black paint and externally covered with backed teflon.

A schematic of the WEB panels with the sizes of the layers is depicted below (Figure 4). The sizing of the WEB thickness is preliminary based on the equivalent conductivity of the resulting multi-layered wall, determined as a function of the thermal conductivity of the involved materials. Interface resistances are not purposely included in the computation to achieve a conservative estimate.

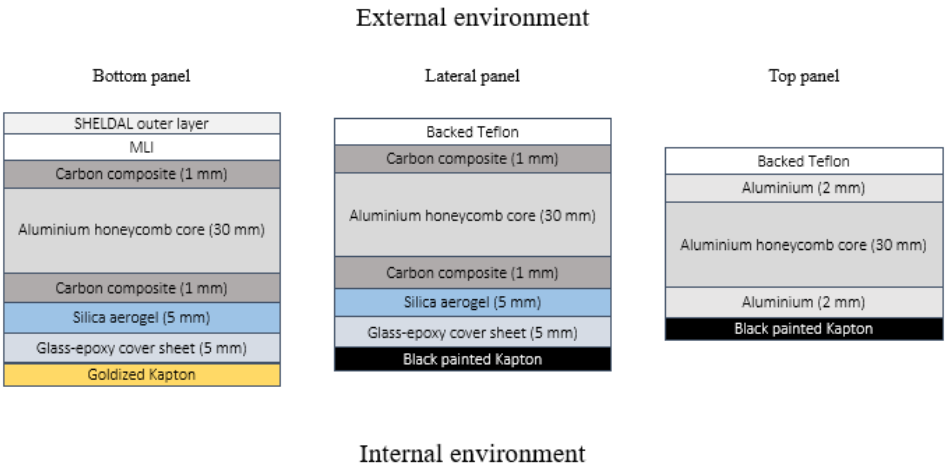

Figure 4: WEB walls schematic cross sections

4.3. Warm motor box panels

The motors rotating the excavating drums are exposed to the external environment, therefore a specific insulation is required to ensure that the proper operating temperatures are maintained. Hence, these motors are enclosed in a modified version of WEB scaled to match the dimensional constraints, referred to as warm motor box (WMB). The WMB provides the structural support required to transmit the loads from the drums to the titanium arm while offering thermal insulation. For the reasons shown above, the bottom panel of the WMB reproduces the same architecture of the WEB bottom panel. The same applies for the top panel, with only one difference, i.e. a white paint replacing the backed teflon. The side panels are instead constituted of a honeycomb structure with aluminum core and carbon

DOI: 10.13009/EUCASS2019-952

composite facesheets, internally covered with black painted Kapton and externally coated with white paint. Table sums up all the optical properties of the external and internal coatings employed both in the WEB and in the WMB.

Table 4: Optical properties of coating surface layers [31]

Coating	Location	α	ε
Goldized Kapton	WEB and WMB bottom panels inside	0.30	0.04
Backed Teflon	Top and lateral WEB panels	0.30	0.40
Black paint	Top and lateral WEB and WMB panels inside	0.95	0.90
White paint	Top and lateral WMB panels	0.25	0.81
Sheldahl coating	MLI outer cover	0.13	0.25

4.4. Active TCS hardware

As it will be shown later in the analysis, the need for additional heating arises during some mission scenarios. In particular, the stand-by mode inside the crater dictates the cold sizing case, requiring 90 W of thermal power to be provided to the system. Different solutions can be adopted, the more reliable being active electric heating. Several types of electric heaters are available, exhibiting a range of properties that easily fulfill the present demand [31]. Electric heaters have high TRL and can be actively tuned allowing for an optimised and responsive thermal control. An alternative to these heat sources is represented by radioisotope heating units (RHUs). RHUs come in different powers and sizes [32] and constitute an extremely durable heat source independent from the power generation subsystem of the vehicle. On the flipside, RHUs cannot be switched off, which implies that additional heat rejection capabilities might be required. Finally, another interesting solution are phase changing materials (PCM).

The tunable properties of these heat capacitors enable a wide range of potential utilisations and a design flexibility that can simplify the optimisation of the thermal control subsystem. Excessive heat generated by the system or by external sources can be stored inside the material and subsequently released during the cold phases at a constant temperature, as a result of the interplay between reversible phase transformations.

Finally, another interesting solution are phase changing materials (PCM).

The tunable properties of these heat capacitors enable a wide range of potential utilisations and a design flexibility that can simplify the optimisation of the thermal control subsystem. Excessive heat generated by the system or by external sources can be stored inside the material and subsequently released during the cold phases at constant temperature, thanks to the interplay between reversible phase transformations. A recommended choice for the present design would be a solid-liquid encapsulated device. Different materials could be used, also to operate under subzero temperatures, like paraffine waxes, acqueous ethylene-glycol solutions-based nanofluids [34], or water-salt eutectic solutions. Here, latent heat of fusion can be as high as 310 kJ/kg [33]. This is not the only parameter that shall be taken into account in performing a selection, as also other factors are important, like the tendency to undergo subcooling of some materials or their stability to repetitive phase transitions. However, these and other drawbacks can be easily mitigated: corrosion of the container can be avoided employing rubber elastic bladders or treating metallic membranes to increase corrosion resistance. The precipitation of solid particles can be reduced adopting eutectic systems. Subcooling phenomena can be tempered introducing cold fingers or nucleating agents. Finally, thermal conductivity can be tuned and increased through the introduction of copper fins [5] or heat transport enhancers [35].

5. Thermal analysis

The thermal control system design is an iterative process where increasingly complex analyses and, later in the project, tests are run in order to verify the fulfilment of temperature requirements of the equipment on board. If not, the design needs to be updated and improved, otherwise it is validated.

In the preliminary phases of the design, when the details of geometry and subsystems are not ready yet, the thermal analyses can be run with some major simplifications. However, even in later phases, the thermal modelling process is an approximation that consists of a mathematical representation of the physical system that can be representative from a thermal standpoint.

The geometry is then meshed and discretized with nodes, isothermal elements characterized by a temperature T_i and a thermal capacitance C_i, and a network of thermal conductors, mainly radiative and conductive. The approach is called lumped parameter network because the continuous parameters of the thermal system are lumped into the discrete set of the nodes [5].

At each node, the following energy equation can be written as:

$$C_i(dT_i/dt) = dQ_{s,i}/dt + dQ_{a,i}/dt + dQ_{p,i}/dt + dQ_{d,i}/dt + \sum_{j=1}^{n} G_{L,ij}\,(T_j - T_i) + \sum_{j=1}^{n} G_{R,ij}\,(T_j^4 - T_i^4) \quad (4)$$

DOI: 10.13009/EUCASS2019-952

Where $Q_{s,i}$, $Q_{a,i}$, and $Q_{p,i}$ are the solar, albedo and planetary thermal loads at i^{th} node respectively, $Q_{d,i}$ is the power dissipated at i^{th} node and $G_{L,ij}$ and $G_{R,ij}$ are the conductive and radiative couplings between nodes. A system of ordinary differential equations is obtained and its numerical solution allows the calculation of the temperature at each node.
The software used for building a geometry and run the simulation is Systema Thermica v4.8.3.
Its application to a given geometric model automatically computes conductive and radiative coupling among the nodes in which the model is subdivided. Then, Equation (4) is solved numerically by the software, with the possibility to study both steady state and transient cases. For thermal control system dimensioning, when there are no strict stability requirements, steady state calculations for the worst hot and cold cases are deemed satisfactory [5]. This is done by setting the left hand side of Equation (4) to zero, resulting in a system of algebraic nonlinear equations that can be solved to obtain the temperature distribution for such extreme cases.
The preliminary results of such analysis are reported in the following sections.

5.1. Identification of worst cases

The combination of heat loads from the external environment and the heat dissipated by the internal electronic equipment let the thermal engineer identify the most critical scenarios. The thermal analysis of the rover is carried out by analysing four scenarios (Table 5): nominal moving, nominal scooping and stand-by inside the crater, and stand-by outside the crater. Since it is still not defined how the charging process will be performed, the charging mode of operation is not included in the thermal analysis.

Table 5: The four scenarios studied with thermal analyses

Environment	**PSR in the crater**			**Outside Crater**
Mode of operation	**Nominal moving**	**Nominal scooping**	**Stand-by**	**Stand-by**
WEB equipment dissipation*	182	114	10	10
WMB equipment dissipation*	0	80	0	0
Solar flux (W/m^2)	0	0	0	1337
Lunar regolith temperature (K)	60	60	60	250

*without active TCS

5.2. Results overview

The thermal analysis for the four scenarios are firstly performed with only a passive TCS, namely WEB and MLI, described in [reference TCS design]. The analyses are then iterated in order to size the amount of heating power required in each scenario. The results are discussed below:

- **Nominal Moving**: The analysis shows that all the equipment predicted temperatures are within its operating temperature limits (Figure 5a). The heating power required to maintain the drum motors within their operating limits, in order to allow them to be instantaneously switched on when scooping is needed, is $22W$ inside each WMB.
- **Nominal Scooping:** The preliminary analysis shows that all the electronics equipment stays within its operating limits, considering uncertainties of $+20°C$, except for the arm motors for which the predicted temperature comes close to design temperature upper limits (Figure 5b). This is due to the fact that, at the present state of analyses, the motors are considered to dissipate the entire amount of electrical power consumed. If this assumption will be confirmed by future studies, the solution would be to increase the conductive coupling between them and the top panel, that acts as a radiator, by means of heat pipes, or to use cooling plates.
- **Stand-By in crater**: This scenario represents the worst cold case for the entire mission, being the rover equipment in stand-by during the exposure to PSR environment. From the analysis (Figure 5c), it is determined that a total heating power required to maintain the equipment within its operating limit is $90W$, with their location distributed among the equipment in order to minimise temperature gradients.
- **Standby outside crater**: The solar flux is here considered impinging the rover on its side. The lowest temperatures are experienced by the motors in the WMBs that are in shadow of the drums (Figure 5d). Moreover, a small amount of heating power is also required for the battery, resulting in $18W$ in total.

DOI: 10.13009/EUCASS2019-952

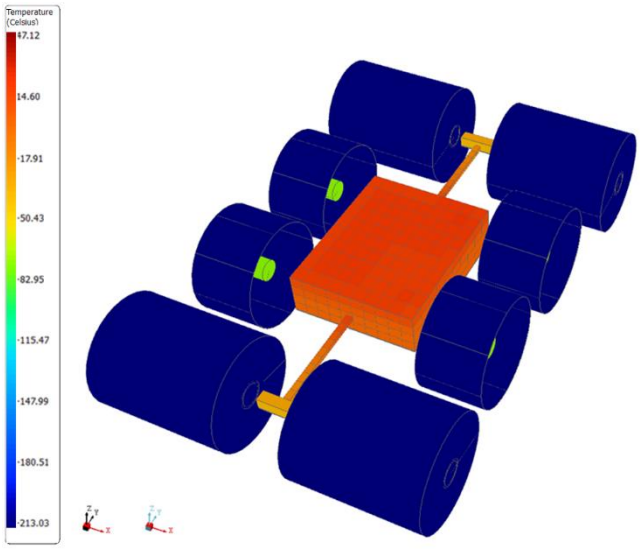

(a-1) Nominal Moving, external

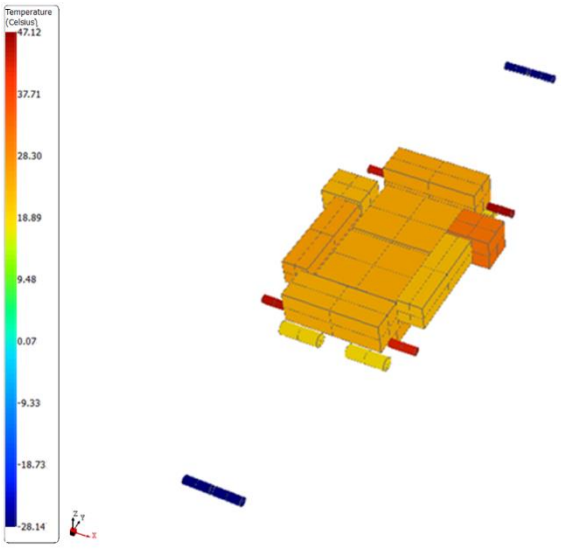

(a-2) Nominal Moving, internal

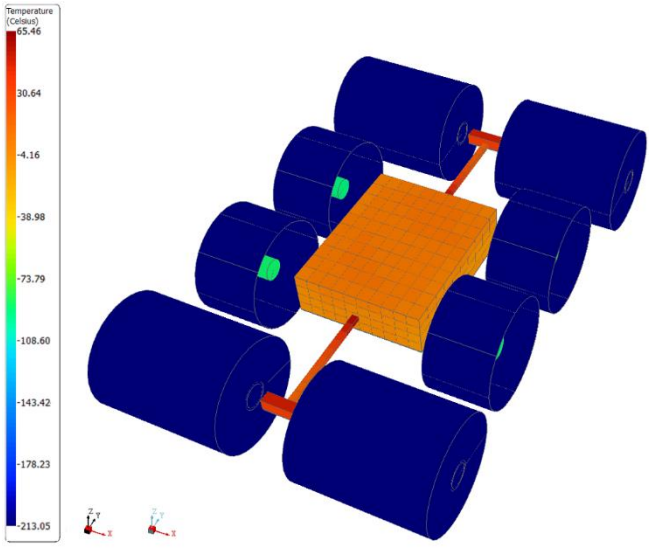

(b-1) Nominal Scooping, external

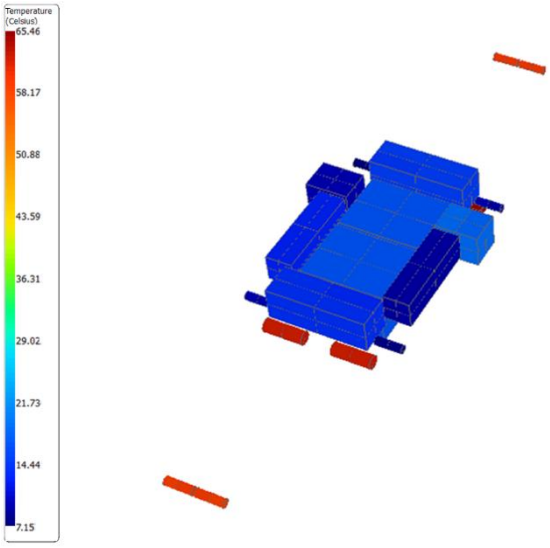

(b-2) Nominal Scooping, internal

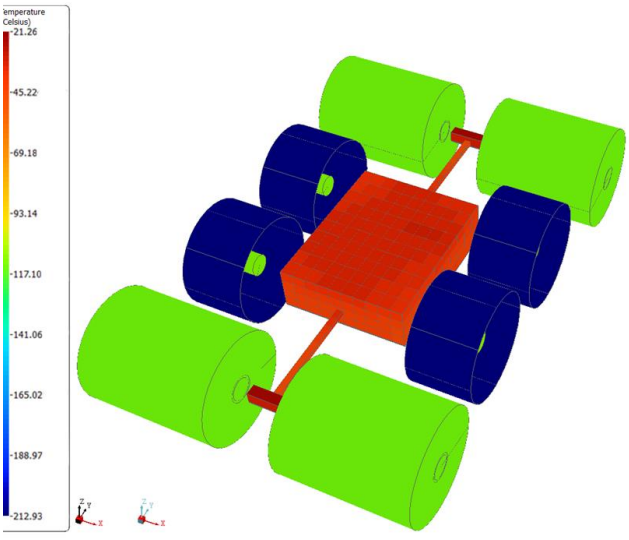

(c-1) Stand-by inside PSR, external

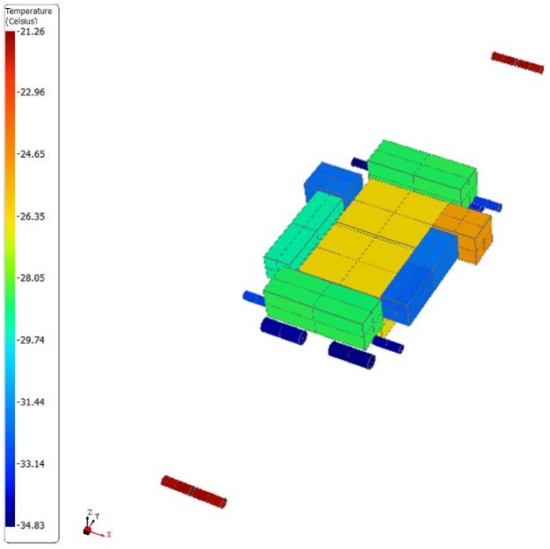

(c-2) Stand-by inside PSR, internal

DOI: 10.13009/EUCASS2019-952

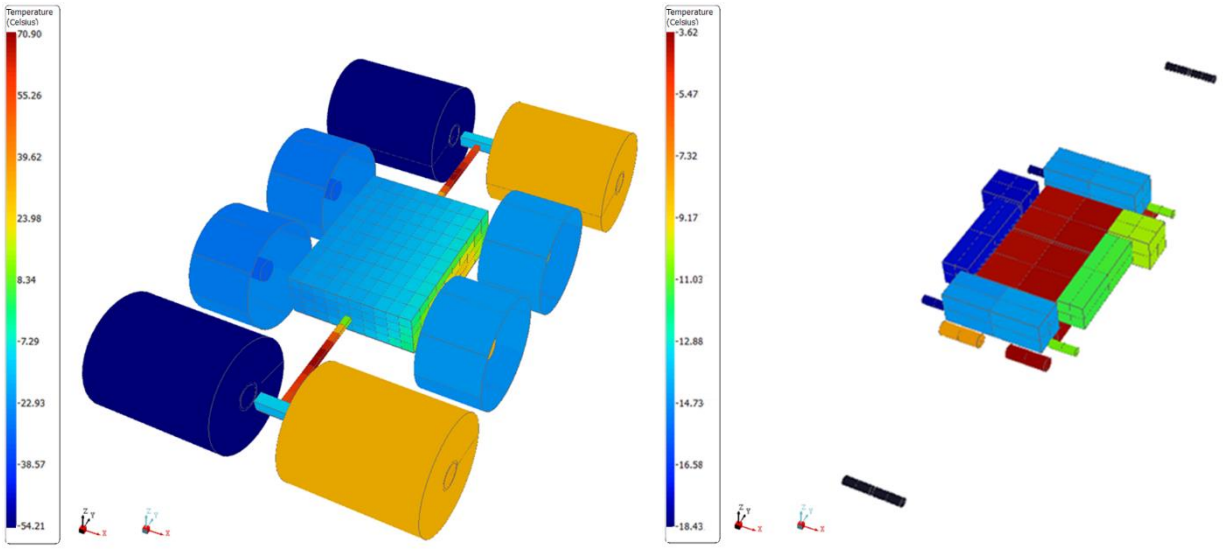

(d-1) Stand-by outside PSR, external (d-2) Stand-by outside PSR, internal

Figure 5: Thermal analysis results overview.

6. Critical technologies

The preliminary thermal analysis performed provides some insights in identifying the most critical technologies. Advancements in these products would significantly increase present-day capabilities and enable new missions. As expected, batteries and general electronics reveal the most delicate pieces of equipment. Battery technology is experiencing constant improvements: NASA Jet Propulsion Laboratory provided demonstration of Li-Ion batteries charging at temperatures as low as -40°C and discharging at -70°C, using special electrolytes developed in-house. Although TRL is still 3, it represents however a promising technology [36].
As regards general electronics, the Low Temperature Electronics Program carried by NASA Glenn Research Center has worked on electrical components capable of operating at -196°C [37].
Mechanical parts also deserve special attention, specifically concerning the operative temperatures of lubricants. Future developments should be addressed at reducing the lower temperature limits for these materials, which would in turn unlock new mobility solutions for exploration vehicles.

7. Future work

The present work established a base ground from which promising future investigations can branch out. More accurate modeling of the system shall be crafted, increasing the number of details included and parts represented, in accordance with a maturing mechanical design. Transient thermal analysis shall be carried as natural prosecution of the stationary baselines outlined up to now, in order to verify the actual reaching of thermal equilibrium as considered in the steady-state analyses. Other techniques capable of increasing the TCS performances shall be explored, such as thermal wrapped insulation, heat straps, heat pipes and more advanced MLI. A trade-off among different heating devices shall be realized. Further detailing of the concept of operation might favour a more realistic rendering of the examined scenarios.
Some of the considerations that may be included in future work also concern more accurate analyses of the dust contamination problem and the inclusion of the heat flux components that were neglected during this analysis. More data about the thermal properties of regolith are needed. In particular, thermal properties for very cold temperatures ($100\ K$) and the thermal interface resistances between regolith and wheels are to be experimentally validated. Similarly, interface resistances among the various materials constituting the system are very difficult data to find in literature, thus a specific test campaign should be addressed to this topic. All these uncertainties may be treated with sensitivity analyses aimed at investigating how the system behaves when the most critical parameters are varied.

DOI: 10.13009/EUCASS2019-952

8. Conclusions

The preliminary results of a thermal analysis of a robotic regolith collection system operating in permanently shadowed lunar regions have been presented. The lunar environment inside the craters entails hard challenges that need to be faced in order to achieve advanced ISRU capabilities. It has been here suggested a starting baseline for the development of an architecture that can unlock this potential by combining configurational, technological and operational solutions. The inclusion of the most critical components inside warm boxes still constitutes the only viable option to carry out these activities successfully. Nonetheless, by carefully planning the operations throughout all the mission phases, it is possible to leverage the power dissipation phenomena to maintain the nominal operating temperatures of the equipment within range, minimising the need for active heating or cooling systems. This peculiar aspect shall emerge as a key driver in future ISRU missions design for its potential to reduce the technological difficulties that up to now played a major role in preventing the exploitation of the resources and opportunities that the Moon holds for humanity. This study has been carried out as part of the Project Work of the international master "SpacE Exploration and Development Systems" (SEEDS) held by three European universities, namely Politecnico di Torino (Italy), ISAE Supaero (France) and University of Leicester (UK), and supported by Thales Alenia Space Italy, Italian Space Agency (ASI) and European Space Agency (ESA).

Acknowledgements

The authors would like to thank Enrico Sacchi (Thales Alenia Space Italy), Andrea Merlo (Thales Alenia Space Italy), Giancarlo Genta (Politecnico di Torino), Davide Barbero (Politecnico di Torino), Lucile Desjonqueres (European Space Agency) and Systema Thermica for the support offered during the realisation of this work.

References

[1] Deans, M., Foessel, D. A., Fries, G. A., LaBelle, D., Lay, N. K., Moorehead, S., ... & Whittaker, W. (1997). *Icebreaker: A Lunar South Pole Exploring Robot*. Carnegie Mellon Tech. Rept., CMU-RI-TR-97-22.

[2] Park, T. Y., Lee, J. J., Kim, J. H., & Oh, H. U. (2018). Preliminary Thermal Design and Analysis of Lunar Lander for Night Survival. International Journal of Aerospace Engineering, 2018.

[3] Whittaker, W. L. (1995). Design of a Day/Night Lunar Rover. Robotics Institute Technical Report CMU-RI-TR-95-24, Carnegie Mellon University, Pittsburgh, PA.

[4] ESA Requirements and Standards Division (2008) Thermal control general requirements, ECSS-E-ST-31C.

[5] Meseguer, J., Pérez-Grande, I., & Sanz-Andrés, A. (2012). Spacecraft thermal control. Elsevier.

[6] Siegler, M. A., Bills, B. G., & Paige, D. A. (2011). Effects of orbital evolution on lunar ice stability. *Journal of Geophysical Research: Planets*, *116*(E3).

[7] Nozette, S., Spudis, P. D., Robinson, M. S., Bussey, D. B. J., Lichtenberg, C., & Bonner, R. (2001). Integration of lunar polar remote-sensing data sets: Evidence for ice at the lunar south pole. *Journal of Geophysical Research: Planets*, *106*(E10), 23253-23266.

[8] Paige, D. A., Siegler, M. A., Zhang, J. A., Hayne, P. O., Foote, E. J., Bennett, K. A., ... & Foote, M. C. (2010). Diviner lunar radiometer observations of cold traps in the Moon's south polar region. *science*, *330*(6003), 479-482.

[9] Birkebak, R. C., & Cremers, C. J. (1974). Thermal Radiation Characteristics and Thermophysical Properties of Lunar Materials, *NASA-CR-139950*.

[10] Hager, P. B. (2013). *Dynamic thermal modeling for moving objects on the Moon* (Doctoral dissertation, Technische Universität München).

[11] Yovanovich, M. M. Thermal interface (joint) conductance and resistance. URL: http://mhtl.uwaterloo.ca/courses_old/ece309/notes/conduction/cont.pdf

[12] Lieng-Huang, L. (1995). Adhesion and cohesion mechanisms of lunar dust on the moon's surface. *Journal of Adhesion Science and Technology*. 9:8, 1103-1124, DOI: 10.1163/156856195X00932

[13] Skonieczny, K. (2013). Lightweight robotic excavation. Ph.D Thesis, Carnegie Mellon University, Pittsburgh, PA, USA URL: http://panda.frc.ri.cmu.edu/projects/lunarExcavator/SkoniecznyThesis.pdf

[14] Mueller, R. P., Smith, J. D., Schuler, J. M., Nick, A. J., Gelino, N. J., Leucht, K. W., ... & Dokos, A. G. (2016). Design of an Excavation Robot: Regolith Advanced Surface Systems Operations Robot (RASSOR) 2.0. In *Earth and Space 2016: Engineering for Extreme Environments* (pp. 163-174). Reston, VA: American Society of Civil Engineers.

[15] NASA. Superelastic Tire. A viable alternative to the pneumatic tire. *URL: https://technology.grc.nasa.gov/patent/LEW-TOPS-99*

[16] David, E. (2003). Materials for cryogenics applications. In 12th International scientific conference on achievements in mechanical and materials engineering, AMME.

DOI: 10.13009/EUCASS2019-952

[17] Hurlich, A. (1968). Low temperature metals. In Proceedings of the 1968 Summer Study on Superconducting Devices and Accelerators (pp. 311-325).
[18] Hübner, W., Gradt, T., Schneider, T., & Börner, H. (1998). Tribological behaviour of materials at cryogenic temperatures. Wear, 216(2), 150-159.
[19] SRE-PA & D-TEC staff. (2012). Margin philosophy for science assessment studies. *URL: http://sci.esa.int/science-e/www/object/doc.cfm?fobjectid=55027*
[20] Saft America, Inc. (2014). MP 176065 Integration TM xtd. *URL: http://biakom.com/pdf/MP176065_Saft.pdf*
[21] Hague, R. (2016). Philae: A made to measure battery. *ESTEC AIM Workshop. URL: https://indico.esa.int/event/133/contributions/749/attachments/828/1005/15_Lessons_learnt_from_Rosetta.pdf*
[22] Phillips, R., Palladino, M., & Courtois, C. (2012, May). Development of brushed and brushless DC motors for use in the ExoMars drilling and sampling mechanism. In Proceedings of the 41st Aerospace Mechanisms Symposium.
[23] Castrol Braycote 601 EF. Grease, Rust Preventive, Rocket Propellant Compatible. *https://www.2spi.com/catalog/documents/451695_US_en.pdf*
[24] Poulakis, P., Vago, J. L., Loizeau, D., Vicente-Arevalo, C., Hutton, A., McCoubrey, R., ... & Otero-Rubio, A. (2015). Overview and development status of the Exomars rover mobility subsystem. Advanced Space Technologies for Robotics and Automation, 1-8.
[25] NASA Quickmap. *URL: https://quickmap.lroc.asu.edu*
[26] Doenecke, J. (1993). Survey and evaluation of multilayer insulation heat transfer measurements (No. 932117). SAE Technical Paper.
[27] Sheldhal, The Red Book SMPB-1007 REV A, *URL*: http://www.sheldahl.com/sites/default/files/Documents/ShieldingMaterials/RedBook.pdf
[28] Gbewonyo, S., Carpenter, A. W., Gause, C. B., Mucha, N. R., & Zhang, L. (2017). Low thermal conductivity carbon fibrous composite nanomaterial enabled by multi-scale porous structure. Materials & Design, 134, 218-225.
[29] Bheekhun, N., Talib, A., Rahim, A., & Hassan, M. R. (2013). Aerogels in aerospace: an overview. Advances in Materials Science and Engineering, 2013.
[30] Silica-based aerogel. *URL: http://www.esa-tec.eu/space-technologies/from-space/silica-based-aerogel/*
[31] Gilmore, D. G. (2002). Spacecraft Thermal Control Handbook, Volume 1: Fundamental Technologies.
[32] Summerer, L., & Stephenson, K. (2011). Nuclear power sources: a key enabling technology for planetary exploration. Proceedings of the Institution of Mechanical Engineers, Part G: Journal of Aerospace Engineering, 225(2), 129-143.
[33] CRISTOPIA Energy Systems. *www.cristopia.com*
[34] Mo, S., Zhu, K., Yin, T., Chen, Y., & Cheng, Z. (2017). Phase change characteristics of ethylene glycol solution-based nanofluids for subzero thermal energy storage. International Journal of Energy Research, 41(1), 81-91.
[35] Lafdi, K., Mesalhy, O., & Elgafy, A. (2008). Graphite foams infiltrated with phase change materials as alternative materials for space and terrestrial thermal energy storage applications. Carbon, 46(1), 159-168.
[36] Surampudi, R., et. al. (2017). Energy Storage Technologies for Future Planetary Science Missions. *URL: https://solarsystem.nasa.gov/system/downloadable_items/716_Energy_Storage_Tech_Report_FINAL.PDF*
[37] Patterson, R. L., Hammond, A., Dickman, J. E., Gerber, S., Overton, E., & Elbuluk, M. (2003). Electrical devices and circuits for low temperature space applications.